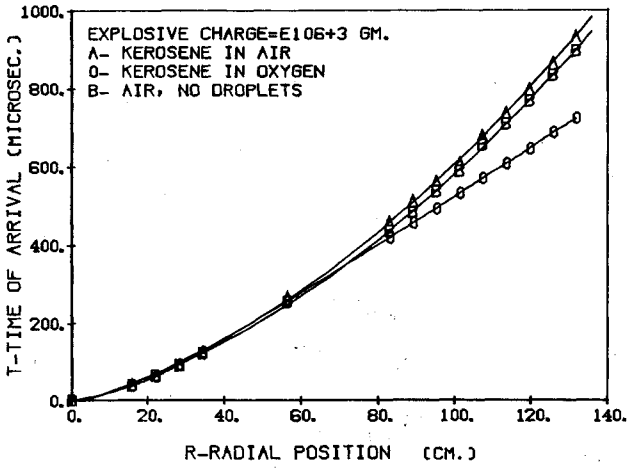

Fig. 2 Blast and detonation waves.

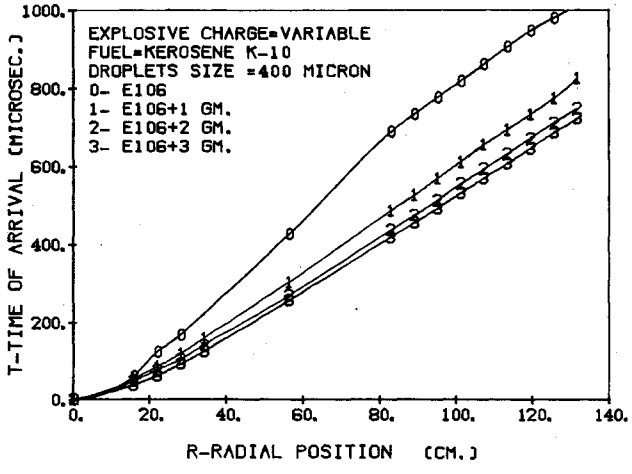

Fig. 3 Detonations of kerosene sprays in oxygen.

decay to a constant velocity, presumably the detonation velocity. Curves 2 and 3 show almost the same velocity of 1560 and 1595 m/s, respectively. Curve 1 reaches a slightly lower velocity of 1450 m/s. In the case of the blasting cap alone, initial decay of the blast wave can be observed but fast acceleration to detonation occurs in the second half of the chamber, and the final velocity seems to be about the same as for the larger charges (1475 m/s). It seems obvious that at larger distances all of those detonation waves will attain the same velocity. The measured velocities in all the runs were 15-22% lower than the theoretical value for an equivalent premixed all gaseous mixture. The lower detonation velocities are attributed in part to heat and drag losses to the walls of the chamber and in part to the incomplete combustion of the liquid droplets.

Further experiments were conducted wherein the kerosene was sensitized by the addition of 25% (by volume) of normal propyl nitrate (NPN). The results are shown in Fig. 4 wherein the energy level was the same for every run. Two curves for the nonsensitized case, shown earlier, are included for comparison. Two separate runs are shown for sensitized kerosene-air. In one case the smooth curve shown indicates constant velocity, or detonation. However, the indicated velocity, 1350 m/s, is low and there is some doubt that detonation occurs. The open circles for the other run, not connected by a curve, are above the curve except at about 115 cm a rapid acceleration of the wave is indicated. It is concluded that this kerosene-NPN-air mixture is close to detonation for this energy level and that higher initiator energies would produce detonation. Finally, the sensitized

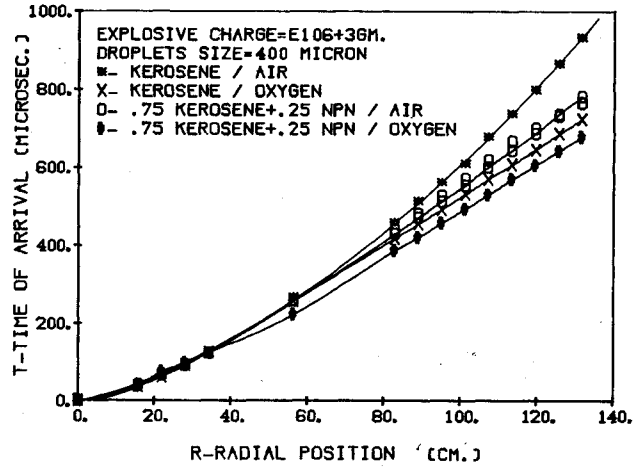

Fig. 4 Effect of the addition of NPN as sensitizer.

kerosene-oxygen mixture is seen to accelerate more rapidly to detonation conditions than in the unsensitized case. The observed velocity of 1660 m/s is again somewhat lower than the theoretical one (1812 m/s) and slightly higher than the nonsensitized case.

Acknowledgment

This research was supported by the U.S. Army Research Office under Grants DAAG29-77-G-0104 and DAAG-29-78-G-0116.

References

[1] Gabrijel, Z. and Nicholls, J.A., "Cylindrical Heterogeneous Detonation Waves," *Acta Astronautica,* Vol. 5, Nov.-Dec. 1978, pp. 1051-1061.

[2] Nicholls, J.A., Sichel, M., Gabrijel, Z., Oza, R., and Vander Molen, R., "Detonability of Unconfined Natural Gas-Air Clouds," presented at the Seventeenth International Symposium on Combustion, University of Leeds, England, Aug. 20-25, 1978; accepted for publication in the proceedings.

[3] Gordon, S. and McBride, B.J., "Computer Program for Calculation of Complex Chemical Equilibrium Compositions, Rocket Performance, Incident and Reflected Shocks, and Chapman-Jouguet Detonation," NASA SP-273, 1971.

J80-110
20016
20018

Axisymmetric Transonic Flow Past Slender Bodies by an Integral Equation Method

N. L. Arora* and J. P. Agarwal†
Indian Institute of Technology, Kanpur, India

Introduction

THE transonic small perturbation equation for inviscid flow past thin airfoils and slender bodies can be transformed into an integral equation for perturbation potential by the application of Green's theorem.[1,2] The integral equation

Received July 27, 1979; revision received Oct. 3, 1979. Copyright © American Institute of Aeronautics and Astronautics, Inc., 1979. All rights reserved.

Index categories: Subsonic Flow; Transonic Flow.

*Professor, Dept. of Aeronautical Engineering.
†Graduate Student.

method has proved quite successful for solving the transonic flow problems of two-dimensional airfoils. The numerical solution to the integral equation has been attempted by various approximate methods (see for examples Refs. 3 and 4), and the solutions are obtained only on the airfoil surface. Nixon[5] and Ogana[6] have extended the computations to the entire flow field.

In the present work, an integral equation suitable for axisymmetric flow past slender bodies of revolution at transonic speeds is obtained. Numerical solution to the integral equation is then sought in the meridian plane by dividing the region of integration into rectangular elements wherein the velocity can be considered uniform. The pressure field is computed on and away from the slender body including the fore and aft body effects. An application to parabolic bodies of revolution with sting is presented at subsonic freestream Mach numbers yielding subcritical and supercritical shock free flows.

Problem Specification

The transonic small perturbation potential equation for axisymmetric flow past a slender body of revolution, Fig. 1, is given by

$$[1-M_\infty^2-(\gamma+1)M_\infty^2\phi_{1x_1}]\phi_{1x_1x_1}+\phi_{1r_1r_1}+\frac{1}{r_1}\phi_{1r_1}=0 \quad (1)$$

Here M_∞ is the freestream Mach number, γ is the ratio of specific heats, x_1 and r_1 are the cylindrical coordinates, and the perturbation velocities $u_1=\phi_{1x_1}$ and $v_1=\phi_{1r_1}$ are normalized by the freestream velocity. The flow tangency condition on the body surface $r_1=R_1(x_1)$ given by the first-order slender body approximation is

$$\lim_{r_1\to 0}(r_1\phi_{1r_1})=R_1\frac{dR_1}{dx_1}=\frac{S'(x_1)}{2\pi},\quad S(x_1)=\pi R_1^2(x_1) \quad (2)$$

In the outer flow, the velocity perturbations must vanish at infinity.

If there are any shocks on the body surface, it is necessary to take into account the discontinuous change in velocities across them. The small perturbation approximation to shock jump conditions gives[2]

$$[(1-M_\infty^2)\langle u_1\rangle-\tfrac{1}{2}(\gamma+1)M_\infty^2\langle u_1^2\rangle]\langle u_1\rangle+\langle v_1\rangle^2=0 \quad (3)$$

where $\langle\ \rangle$ represents a jump in the quantity across the shock.

Finally, the pressure coefficient on the body surface is given by the slender body approximation

$$C_P=-2\phi_{1x_1}-(dR_1/dx_1)^2 \quad (4)$$

Analyisis

For subsonic freestream Mach numbers, it is convenient to introduce the transformations

$$x=x_1,\quad r=\beta r_1;\quad \text{and}\quad \phi=(k/\beta^2)\phi_1 \quad (5)$$

where $\beta=(1-M_\infty^2)^{1/2}$ and $k=(\gamma+1)M_\infty^2$. Using Eq. (5), Eqs. (1-3) become

$$\phi_{xx}+\phi_{rr}+\frac{1}{r}\phi_r=\phi_x\phi_{xx}=\frac{\partial}{\partial x}(u^2/2) \quad (6)$$

$$r\phi_r=(k/\beta^2)\frac{S'(x)}{2\pi}\quad \text{as } r\to 0 \quad (7)$$

$$[\langle u\rangle-\tfrac{1}{2}\langle u^2\rangle]\langle u\rangle+\langle v\rangle^2=0 \quad (8)$$

where $u=\phi_x$ and $v=\phi_r$.

We apply Green's theorem to the flowfield of Fig. 1. If ϕ and ψ are two single-valued functions that are finite and continuously differentiable in the volume V bounded by the surface S, then

$$\iiint_V[\psi L(\phi)-\phi L(\psi)]\,dV=\iint_S\left(\phi\frac{\partial\psi}{\partial n}-\psi\frac{\partial\phi}{\partial n}\right)dS \quad (9)$$

where $\partial/\partial n$ denotes the directional derivative normal to the surface S directed inward to volume V, and L is the Laplacian operator.

Here we identify ϕ with the function satisfying Eq. (6) and let the auxiliary function ψ satisfy $L(\psi)=0$, which has the fundamental solution

$$\psi=1/(4\pi R),\ R=[(x-\xi)^2+r^2+\rho^2-2r\rho\cos(\theta-\nu)]^{1/2} \quad (10)$$

where we have used cylindrical coordinates, and ξ, ρ, and ν are the running variables. Then Eq. (9) simplifies to

$$\iiint_V\psi\frac{\partial}{\partial\xi}(u^2/2)\,dV=\iint_S\left(\phi\frac{\partial\psi}{\partial n}-\psi\frac{\partial\phi}{\partial n}\right)dS \quad (11)$$

It must be observed that ψ is singular at $R=0$; u and $\partial\phi/\partial n$ are discontinuous across the shock, while ϕ, ψ and $\partial\psi/\partial n$ are continuous there. Thus Eq. (11) can be applied to region V bounded by surface S which includes the cylindrical surface S_C at infinity, the small spherical surface S_P surrounding the singular point (x,r,θ), the surface S_D around any shock discontinuity, and the body surface S_B.

Without any loss of generality we may take $\theta=0$ for axisymmetric flow. The surface integral over S_P can be evaluated to yield $-\phi(x,r)$. The integral over the cylindrical surface S_C vanishes with the assumption that $r\to\infty$, $\phi\sim R^{-\epsilon}$, $\epsilon>0$. The integral over the body surface is evaluated by noting that for small r, $\phi\sim S'(x)\ell nr+g(x)$. Finally, taking into account the shock jump condition [Eq. (8)], Eq. (11) can be shown to yield an integral equation for ϕ

$$\phi(x,r)=\phi_B(x,r)+\iiint_V\frac{u^2}{2}\frac{\partial\psi}{\partial\xi}\,dV \quad (12)$$

with

$$\phi_B=-(k/\beta^2)\frac{1}{4\pi}\int_0^\ell S'(\xi)[(x-\xi)^2+r^2]^{-1/2}d\xi$$

Here ℓ is the body length, and ϕ_B is the linear value of the perturbation potential for subsonic axisymmetric flow past slender bodies. The integral equation for an axial velocity perturbation u is obtained by differentiating Eq. (12) with respect to x. Thus,

$$u(x,r)=u_B(x,r)+\frac{1}{4\pi}\frac{\partial}{\partial x}\int_{-\infty}^{\infty}\int_0^{\infty}\int_0^{2\pi}\times\frac{u^2}{2}(\xi,\rho)\frac{\partial}{\partial\xi}(1/R)\rho\,d\nu\,d\rho\,d\xi \quad (13)$$

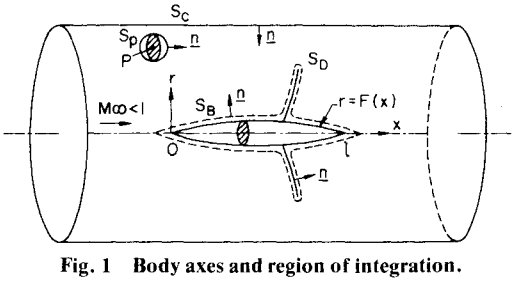

Fig. 1 Body axes and region of integration.

Numerical Solution

The region of integration in the meridian plane is divided into rectangular elements containing the grid point (x_i, r_j). It is assumed that the velocity $u(\xi,\rho)$ within each element can be represented by its value at the grid point. Then, taking appropriate care of the singular behavior of the integrand, Eq. (13) can be expressed in summation form as

$$u(x,r) = u_B(x,r) + \sum_{i,j} a_{ij}(x,r)\, u^2(x_i, r_j) \tag{14}$$

with

$$a_{ij} = -\frac{1}{8\pi}\int_{x_i-\delta_i}^{x_i+\delta_i}\int_{r_j-h_j}^{r_j+h_j}\int_0^{2\pi} \rho \frac{\partial^2}{\partial \xi^2}(1/R)\,\mathrm{d}\nu\mathrm{d}\rho\mathrm{d}\xi$$

$$= \frac{1}{2\pi}\{E[K(X_1)]G(X_1)H(X_1) - E[K(X_2)]G(X_2)H(X_2)\}$$

Here $E[K(X)]$ is the complete elliptic integral of second kind, and

$$K(X) = \{4rr_j/[X^2 + (r+r_j)^2]\}^{1/2},$$

$$G(X) = r_j/[X^2 + (r+r_j)^2]^{1/2}$$

$$H(X) = \arctan[(r_j - r + h_j)/X] - \arctan[(r_j - r - h_j)/X]$$

$$X_1 = x - x_i + \delta_i,\ X_2 = x - x_i - \delta_i$$

Now solution of Eq. (14) is sought by iteration, which in subscripted form is

$$u_{sp}^{(n)} = (u_B)_{sp} + \sum_{i,j} a_{ijsp}\,(u_{ij}^2)^{(n-1)} \equiv g \tag{15}$$

where the superscript (n) indicates the nth iterative step. A faster convergence is achieved by adding $-u_{sp}\,\partial g/\partial u_{sp}$ to both sides of Eq. (15). The initial value is taken to be $u_{sp}^{(0)} = (u_B)_{sp}$, whereas the successive iterates are defined as

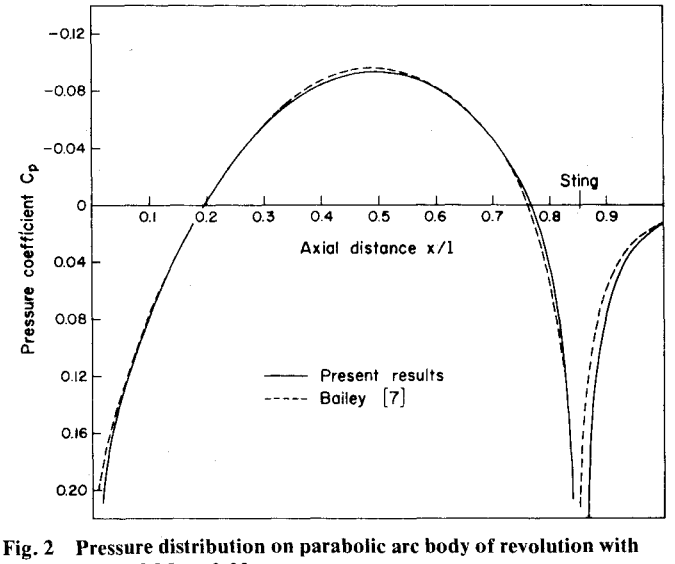

Fig. 2 Pressure distribution on parabolic arc body of revolution with sting; $f = 10$ and $M_\infty = 0.90$.

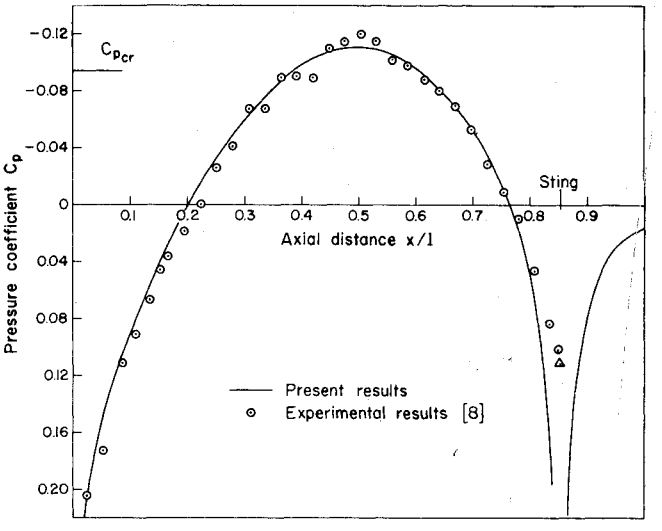

Fig. 3 Pressure distribution on parabolic arc body of revolution with sting; $f = 10$ and $M_\infty = 0.95$.

$$u_{sp}^{(n)} = \Big[(u_B)_{sp} - 2a_{spsp}(u_{sp}^2)^{(n-1)} + \sum_{i,j} a_{ij}(u_{ij}^2)^{(n-1)}\Big] \Big/ (1 - 2a_{spsp}u_{sp}) \tag{16}$$

Results and Discussion

Calculations are made for a parabolic arc body of revolution of fineness ratio $f = 10$ with sting at 0.854 ℓ at freestream Mach numbers $M_\infty = 0.90$ (subcritical) and $M_\infty = 0.95$ (supercritcal shock free). The integration was carried out in the range $-0.28 \le x/\ell \le 1.16$ and $0 \le r/\ell \le 1.1$ using 37×6 rectangular elements with streamwise grid size $\Delta x/\ell = 0.04$. Converged solutions were obtained in 4 to 7 iterations. The results for C_P distribution on the body surface for $M_\infty = 0.9$ are shown in Fig. 2 and compared with Bailey's results[7] obtained by finite-difference solution of the transonic small disturbance equation using a network of 109×50 grid points. Excellent agreement is achieved on the body ahead of the sting. The results for $M_\infty = 0.95$ on the body surface are compared with the experimental results of Taylor and McDevitt[8] in Fig. 3. The comparison shows generally good agreement.

References

[1] Spreiter J. R. and Alksne, A. Y., "Theoretical Predictions of Pressure Distributions on Nonlifting Airfoils at High Subsonic Speeds," NACA Report 1217, 1955.

[2] Heaslett, M. A. and Spreiter, J. R., "Three-Dimensional Transonic Flow Theory Applied to Slender Wings and Bodies," NACA Report 1318, 1957.

[3] Nφrstrud, H., "The Transonic Airfoil Problems with Embedded Shocks," *The Aeronautical Quarterly,* Vol. 24, Pt. 2, 1973, pp. 129-138.

[4] Nixon, D. and Hancock, G. J., "High Subsonic Flow Past a Steady Two-Dimensional Aerofoil," ARC CP 1280, 1974.

[5] Nixon, D., "Extended Integral Equation Method for Transonic Flows," *AIAA Journal,* Vol. 13, July 1975, pp. 934-935.

[6] Ogana, W., "Numerical Solution for Subcritical Flows by a Transonic Integral Equation Method," *AIAA Journal,* Vol. 15, March 1977, pp. 444-446.

[7] Bailey, F. R., "Numerical Calculation of Transonic Flow about Slender Bodies of Revolution," NASA TN-D 6582, 1971.

[8] Taylor, R. A. and McDevitt, J. B., "Pressure Distribution at Transonic Speeds for Parabolic Arc Bodies of Revolution Having Fineness Ratios of 10, 12 and 14," NACA TN 4234, 1958.